International Journal of Research
Available at https://journals.pen2print.org/index.php/ijr/
e-ISSN: 2348-6848
p-ISSN: 2348-795X
Volume 06 Issue 07
June 2019

An Effective Method to Eliminate the Input Current Harmonics of Matrix Converter by Feedback Control under Unbalanced Input Voltages

Busaramanu Balaji & S.Rama Maddilety
[1]P.G. Scholar, [2]Associate. Professor
[1,2] Dept. of EEE.
[1,2] SVR ENGINEERING COLLEGE
[1,2] NANDYAL, Kurnool Dist. A.P.
Email:- balaji.baalu@gmail.com

ABSTRACT

It is generally considered that feedback control of input currents in the matrix converter (MC) is hard to be realized due to the coupling of input control and output control, which reduces the degree of freedom and robustness. Moreover, under unbalanced input voltages, the coupling also results in severe distortion of input currents when the commonly used feedforward compensation control method with fixed input power factor is adopted. To address these two issues, this project proposes a feedback control strategy on the input side of MC. This strategy is based on a control method which can modify input reference currents. The input control strategy is embedded into the output control strategy and thus is the inner-loop of the system control. The input-side controllers can be designed to achieve expected input control objectives and maintain the output performance at the same time.

On this basis, resonant controllers are applied to regulate input currents and instantaneous active power, so as to directly eliminate the input current harmonics and meanwhile ensure the load absorbing constant active power under unbalanced input voltages. The validity and feasibility of the proposed strategy is verified by the simulation and experimental results.

Keywords:- Matrix Converter,

INTRODUCTION:

Matrix Converter (MC) is a direct AC-AC power converter, featuring no energy storage elements on the dc bus. Compared with back-to-back (B2B) voltage source converter, MC has the advantages of smaller volume and lighter weight [1-2], and has been applied to motor drives [3], unified power flow controller [4], distributed generation system [5], etc.

Due to the lack of energy storage elements on the dc bus, the input control and output control of MC are closely coupled [6]. A general opinion in literature is that the coupling leads to a lower degree of freedom and less robustness of MC than the B2B converter [1, 6]. This is because the phase angle of input current vector can be predetermined, but the amplitude has to adjust itself passively through the load current segments [1, 6].

Therefore, the input current control is not directly controlled and MC doesn't allow for feedback control of input currents. Reference [7] tried to apply closed-loop control based on PID controllers to the regulation of input currents. However, the authors of [7] then found that the feedback control on the input side turned out to be conflicted with that on the output side [8], which could degrade output performance and thus was of low practical value.

On the other hand, the input-output coupling enables the input disturbances to be transferred directly to the load, thereby influencing the waveform quality on the output side. In practical application, the utility grid usually serves as the power supply of MC and thus input voltages are likely to be unbalanced due to the numerous asymmetric loads in the power grid. To avoid low-order

International Journal of Research
Available at https://journals.pen2print.org/index.php/ijr/
e-ISSN: 2348-6848
p-ISSN: 2348-795X
Volume 06 Issue 07
June 2019

harmonics in output currents resulting from input unbalance, the input control and output control need to coordinate with each other [9].

The most common control method in practice is the feed forward compensation of input voltage amplitude [10]. In this method, the real-time values of three-phase input voltages are measured to calculate their instantaneous amplitude.

Then the modulation index of MC is corrected according to the obtained input voltage amplitude. Besides, the input power factor angle is usually fixed at a constant value (e.g. 0 to achieve unit power factor operation). Reference [11] proved that this common method would result in considerable 3rd, 5th, and other odd order harmonics in input currents when the input voltages were unbalanced. Consequently, the highly distorted input currents lead to poor quality of power supply.

Therefore, it is necessary to reduce input current harmonics of MC under unbalanced input voltages. Reference [11] proposed an improved control method which dynamically modified the input power factor angle according to the positive and negative sequence components of input voltages, rather than fixing it at a constant value.

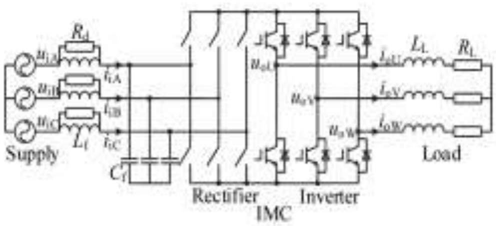

Fig 1.1 structure of MC system

Simulation and experimental results [11-13] demonstrated that this improved control method could obtain sinusoidal input currents when input voltages are unbalanced, while doesn't influence the waveform quality of output currents. The idea of this method is adopted by some researchers.

Similar control methods for sinusoidal input currents were realized in [14-15] based on enhanced double-line voltage synthesis algorithm, in [16] with online optimization of duty cycles, and in [17] utilizing mathematical construction method. In addition, reference [17] showed that if the input current vector angle was only imposed along the positive sequence vector of input voltages, the harmonics content of input currents was less than the conventional control method presented in [10] but larger than the improved method in [11]. Reference [18] simplified the realization of the improved method in [11], which only needed a notch filter to obtain the expected input power factor angle. Yet, most of these methods were highly dependent on the sequence decomposition algorithms and/or input voltage sampling.

In voltage source converters, it is common to eliminate input current harmonics under unbalanced input voltages by incorporating resonant controllers into the closed-loop control method of input currents [19].

However, there is no corresponding achievement for MC due to the general opinion that feedback control of input currents is difficult to realize. Reference [20] presented a control method for MC which could directly control input currents without affecting the output performance. This control method enables the realization of a novel active damping control strategy of equivalent damping performance with passive damping control. Based on the method in [20], a feedback control strategy on the input side of MC is proposed in this paper.

This strategy includes closed-loop control of input currents and input active power. In this control strategy, resonant controllers are adopted to regulate input currents and active power, so as to eliminate the input current harmonics directly and keep the active power constant as required by load. Compared with the conventional control method, the proposed method can improve the waveform quality of input currents dramatically without degrading the waveform quality of output currents.

MATRIX CONVERTERS

Introduction To Two Stage Converter:

International Journal of Research
Available at https://journals.pen2print.org/index.php/ijr/
e-ISSN: 2348-6848
p-ISSN: 2348-795X
Volume 06 Issue 07
June 2019

The two stage AC-DC-AC converters with the voltage source or the current source based on PWM are conventionally used to produce variable frequency output voltage from the constant frequency AC supply system for variable speed drive applications. However, these two stage converters end with poor efficiency, the higher maintenance cost of energy storage elements, reduced high-performance lifetime by the use of large energy storage elements in the DC link, lower order harmonics and suffers from the lack of bidirectional power flow capability through deceleration. Figure 3.1 shows the conventional type Voltage Source Inverter (VSI) fed induction motor drive, where a heavy energy storing capacitor is present which makes them system costly, reduces the energy density and lifetime of the scheme.

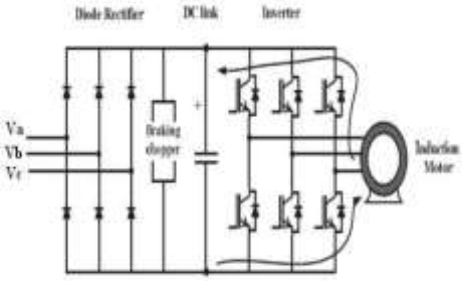

Figure 2.1 Structure of Voltage Source Inverter

It is a two-stage converter that reduces the efficiency of the device. The DC-link capacitor addresses another weak point of the indirect conversion scheme using electrolytic capacitors having high energy storage capability but also a high-temperature sensitivity which decreases their lifetime, as presented by Marco Matteini (2001) as shown in Figure 3.2, calculating higher maintenance costs of the conversion system. It should be found out that the electrolytic capacitor has less lifetime of any element, active or passive, used in power electronic converters as addressed by Mohan et al. (1995)

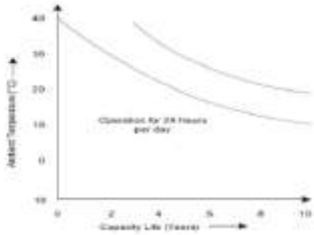

Fig 2.2 capacitor lifetime expectations depending on the ambient temperature in a low power industrial diode bridge VSI

Introduction To Matrix Converters

MCs are useful in high power generation like wind energy, solar energy, and Unified Power Quality Control (UPQC) systems Kandasamy.K.V (2015). Such circuits are easily adaptable where critical power situation occurs. The two most popular known types of renewable energy systems are PV and the wind energy systems. As the power received from the wind energy system is in the form of AC source the efficient power conversion is inevitable. There are various power conversion systems such as the AC/AC, AC/DC/AC, AC/DC. MC systems are of two types, DMC and IMC. As in the case of theVSI, there is the need of the heavy DC-link capacitors used for the power conversion as well as it acts as the storage element. Matrix type AC-DC-AC conversion systems do not require storage element. Another merit of the MC is the no extra components for diode rectifier, filters, and charge-up circuits are required.

The DMC achieve the voltage and current conversion on the single stage. However, in IMC, the VSI category power conversion takes place without the use of the additional capacitor bank. Thus, the system does not require storage element in between load and source side. The MC has various applications together with variable speed drives due to the reduction of power semiconductors used, the cost of the overall system is reduced. Figure 3.3 shows the DMC topology with the single stage of power conversion Kolar J.W et al.(2002).

CMC and IMC, both compared to high-frequency link offshore WECSs. The CMC of low rating IGBT switches in series as well as in

e-ISSN: 2348-6848
p-ISSN: 2348-795X
Volume 06 Issue 07
June 2019

the parallel connections has been established efficient compared to the IMC in CSR and VSI configurations Nathalie Holtsmark et al. (2011). The dual bridge MC topologies can be used to decrease the number of switches from eighteen to nine for the unidirectional power flow applications Wei .L et al. (2002).

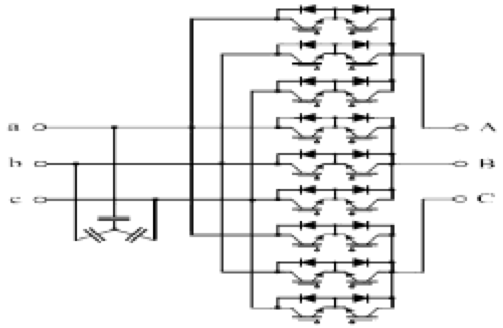

Fig 2.3 Conventional Direct Matrix Converter

The VAWT has the advantage of the removal of heavy nacelle or yaw system Aravind. C.V and Ramesh, G.P (2013). A significant amount of kinetic energy that can be extracted is 59.3% by the Betz limitations for converting the mechanical input to the usable kinetic energy Ramesh. G.P and Aravind. C.V, (2015). There are various closed loop control techniques implemented using power semiconductors, for decreasing the cost of energy and maximize the overall system efficiency.

The structure of CMC is shown in Figure 3.3. The MC is a single-stage converter which directly connects between one phase of the input and one phase of the output without the need for intermediate energy storage components Hulusi. K' and Ramazan. A (2010) that has an array of m by n bi- directional switches which directly connects m-phase input voltage source to the n-phase load. It is a single stage, direct AC-AC converter without the need of energy storage elements in power stage and also a pure silicon converter.

This topology of AC-AC converter was first introduced by Gyugyi and Pelly to obtain an unlimited output frequency. In 1980, generalized high- frequency switching strategy was proposed by Venturini, (1980) and this single stage converter was named as MC. Traditionally AC voltages and currents having the variable amplitude or variable frequency or indirectly obtained by using rectifier DC link inverter system. Indirect power conversion is performed by converting AC-DC and then converting DC back to AC. The matrix converter converting directly from AC-AC been intensely studied as an alternative to conventional indirect power converter systems in recent years due to its following advantages Andreu J et al, (2008), Huber. L and. Borojevic D (1995), Lee K B and Blaabjerg F, (2008) and Wheeler P W et al. (2008).

- Sinusoidal input and output currents
- Four quadrant operation
- Regeneration capability
- Compact design due to the lack of DC links equipment for energy storage.

These above features carrying to study the MC. The load side MC is directly affected by the distorted and distortion input voltages due to the lack of DC intermediate circuit in the MC.The working performance of the load has deteriorated, when it is exposed to the harmonic and non-sinusoidal currents. If unfavorable effects of the distorted input voltage are removed the MC; the popularity of the MC can increase more studies on distorted or unbalanced input voltages Nielsen P et al., (1996), Sun.K et al., (2004) and Sünter S et al. (2009).

Three phase to three phase DMC is given in Figure 3.4**.** The MC is characterized by its ability to connect any input phase to any output phase at any instant. This allows bi-directional power flow and sinusoidal input currents by directly interconnecting the input and output voltage systems through bi-directional switches. MC has numerous advantages such as no DC link capacitor or inductor, sinusoidal input current and output voltage, possible power factor control, four-quadrant operation, compact and straightforward design and energy regeneration

e-ISSN: 2348-6848
p-ISSN: 2348-795X
Volume 06 Issue 07
June 2019

capability. The disadvantages are the need for many bi-directional switches, increased complexity of scrutiny, the complex of bidirectional switches and sensitivity to input voltage disturbance

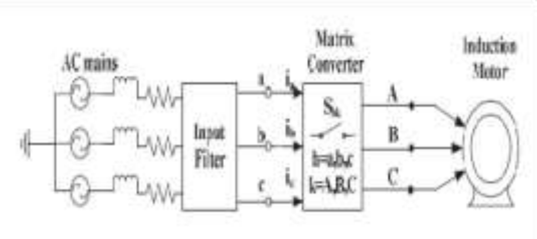

Fig 2.4 Structure of Matrix Converter

Figure 3.5 shows the different types of AC- AC power converters for WECS. The three basic topologies of MC are the converter with DC link storage, hybrid MC, and MC then some extended topologies depend on upon some bidirectional switches and diodes used for direct power conversion.

This thesis is proposed using USMC for WECS.

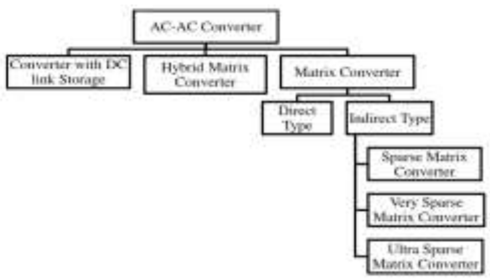

Fig 2.5 Different types of AC – AC power converter

Direct Matrix Converter

The basic configuration of three phase to three phase DMC was introduced by Venturini (1980). It consists of nine bidirectional switches that connect each output phase to each input phase. Bidirectional switches are configured from back to back connected unidirectional switches. A bidirectional switch is capable of conducting currents and blocking voltages of both polarities, depending on control signal Burany (1989) and thus it must be realized by the combination of conventional unidirectional semiconductor devices. Figure 3.6 shows different bi-directional switch configurations which have been used in prototype and proposed in the literature. Filter capacitors are connected at the input side to facilitate free commutation of current. Different filter types used in MC are shown in Figure 3.7.

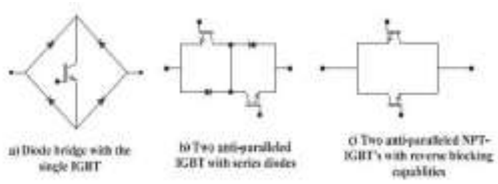

Fig 2.6 Bidirectional switch configurations

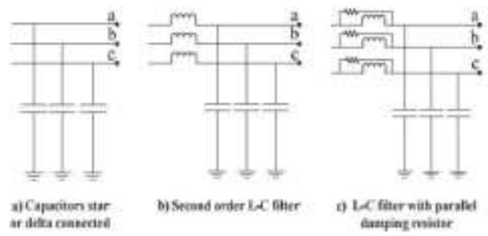

Fig 2.7 Input filter types

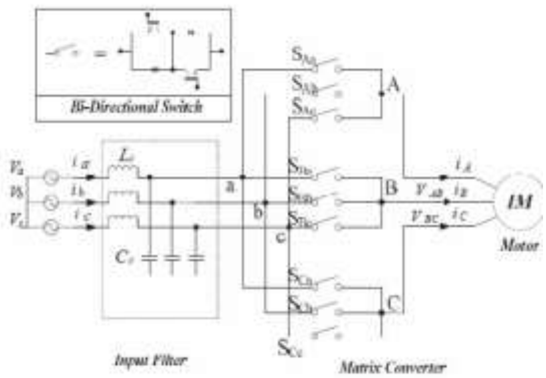

Fig 2.8 Direct matrix converter topology

DMC with nine bidirectional switches is shown in Figure 3.8. The symbol Sij (i=a, b, c and j=A, B, C) represents the ideal bidirectional switches, where i represent the index of the output voltage and j represents the index of the input voltage.

$$V_i = V_{im}\begin{bmatrix}\cos(\omega_i t)\\ \cos\left(\omega_i t - \frac{2\pi}{3}\right)\\ \cos\left(\omega_i t - \frac{4\pi}{3}\right)\end{bmatrix}$$

Let $[V_o]$ be the vector of output voltges

$$V_o = V_{om}\begin{bmatrix}\cos\omega_o t\\ \cos\left(\omega_o t - \frac{2\pi}{3}\right)\\ \cos\left(\omega_o t - \frac{4\pi}{3}\right)\end{bmatrix}$$

$$V_o = [M][V_i]$$

e-ISSN: 2348-6848
p-ISSN: 2348-795X
Volume 06 Issue 07
June 2019

While input and output currents related as

$$[I_i] = [M]^T[I_o]$$

output current I_o are related during commutation, the bidirectional switches must function according to the following rules.

- Any two input phase voltages should not be connected to the same output line to avoid a short-circuit condition.
- Any output phase should not be opened to prevent the interruption of inductive loads.

$$S_{ij}(t) = \begin{cases} 1, & S_{ij}\ \text{closed} \\ 0, & S_{ij}\ \text{open} \end{cases}$$

Where, $i \in \{a, b, c\}$, $j \in \{A, B, C\}$

$$S_{aj} + S_{bj} + S_{cj} = 1;\ j \in \{A, B, C\}$$

the three by three MC can allow only 27 possible switching states among the
512 switching combinations. At every instant t, only one switch only one switch Sij (j = a, b, c) works to ensure a closed loop load current. The switching frequency fs=ωs/2π must have a value twenty times higher than the maximum of fif0 (fs>>20× Max (fif0)).
During the period T known as a sequential period which is equal to 1/fs, the sum of the time of conduction being used to synthesize the same output phase must be equal to Ta. Now a time tij called time of modulation can be defined

2.3.1 INDIRECT MATRIX CONVERTER:

The basic concept of the IMC is to separate the AC/AC conversion into two stages such as rectifier and inverter stages with no DC link capacitor. The rectifier stage is composed of six bi-directional switches built with twelve unidirectional switches, while the inverter stage has six unidirectional switches. As a result, independent switching modulation strategies can be used for each stage. The purpose of the rectifier is generating the sinusoidal input currents as well as maintaining a constant local-averaged dc output voltage in the DC-link, by modulating the two line-to-line input voltages. Output voltages with variable frequency and variable amplitude can be obtained through the conventional space vector PWM modulation of the inverter stage, using the constant DC voltage obtained from the rectifier stage. Alireza jahangiri (2013).
The input LC filter is installed to filter out high-frequency PWM components of the input currents Sangshin Kwak, (2007). Lixiang Wei and Thomas Lipo, (2001) proposed a modified MC topology known as IMC. The IMC topology is shown in Figure 3.9.

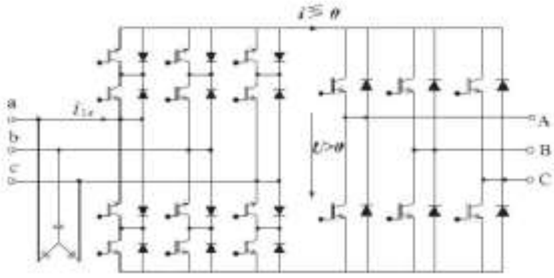

Fig 2.9 Indirect matrix converter topology

Figure 3.9 shows the IMC Topology for WECS. However, to make a sure proper operation of this converter, the DC side voltage should be constantly positive. Rectifier on the line side has similar to the traditional one except for switches all are bidirectional. To maintain pure sinusoidal input current waveforms and to maintain the positive voltage on the DC side are the main objectives of the rectifier. Dissimilarity of the AC/DC/AC converter, the DC capacitors are put back by a small filter on the line side.
For analysis, converters switching frequency are greater than the fundamental frequencies of the both input voltage source and output current source. The input voltage and output current of the switching cycle are assumed constant. Stiff voltage source on the line side and stiff current sink on the output side are assumed. Input voltage and switching functions of the rectifier decides the DC side voltage. The combination of the output switching functions and output current determines the DC side current.

e-ISSN: 2348-6848
p-ISSN: 2348-795X
Volume 06 Issue 07
June 2019

$$V_{sa} = V_m \cos\theta_a = V_m \cos(\omega_i t)$$
$$V_{sb} = V_m \cos\theta_b = V_m \cos\left(\omega_i t - \frac{2\pi}{3}\right)$$
$$V_{sc} = V_m \cos\theta_c = V_m \cos\left(\omega_i t + \frac{2\pi}{3}\right)$$

Equation shows the load current on the load side. Where, ω_0 and ω_i are the input and output angular frequencies. Φ_0 is the initial electric angle of the A phase output current. V_m, I_0 are peak amplitudes of an input voltage, andoutput current respectively.

The converter has the following advantages.

- The performance of the USMC is similar to the fulfillment of the conventional MC, such as better voltage transfer ratio, four-quadrant operation, unity input power factor and pure sine waveforms having both input current and output voltage in the presence of harmonic.
- Control circuit for the USMC is simplified due to PWM algorithms of the conventional inverters.
- All the switches have zero current at the line side turn on and turn off. Hence, USMC does not practice the commutation problems of a CMC.
- USMC does not require energy storage component. Production of small in AC filters is compactly integrated with the system package.

Sparse Matrix Converter Topology:

Kolar et al. (2007) have proposed a novel three-phase AC-AC SMC having no energy storage elements using 15 IGBT switches. For the IMC, a conventional voltage source- type inverter is fed by a four-quadrant switch, current source- type rectifier, which can operate on both positive and negative DC for a unipolar DC-link voltage as required by the inverter stage.

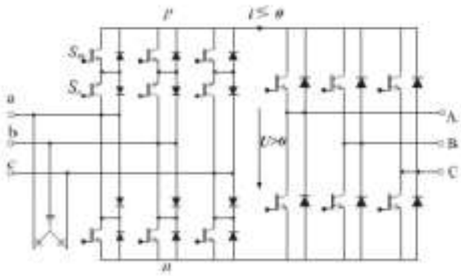

Fig 2.10 Sparse Matrix Converter

The IMC use 18 unipolar turn-off power semiconductors and 18 diodes. Hence, have same realization effort as the CMC. However, the inverter stage can employ a conventional six-pack power module and therefore, this would slightly cut the insight effort compare to a completely discrete CMC. The DC- link voltage of the IMC requires constant polarity. However, the IMC four- quadrant switch current-source-type rectifier can operate with both positive and negative DC-link voltage polarities.

Therefore, the ways of reducing difficulty in the rectifier stage circuit are considered, and the reduction in the number of unipolar turn-off power semiconductors establishing step-by-step for a bridge single leg is given in the Figure 3.10. Therefore, the functionality of the IMC and/or CMC can be realized from the converter topology as depicted in the Figure 3.10

SMC topology utilizes 15 IGBTs, compared to 18 IGBTs of the IMC, and therefore the converter topology is designated as SMC. SMC was representing as an attractive alternative to the CMC for industrial applications. The functionality of a conventional three-phase AC-AC MC can be achieved by employing 15 IGBTs using SMC concept. Zero DC-link current commutation also allows the input stage of an IMC to be realized by four- quadrant switches.

In certain applications, such as aircraft actuators and elevator drives, specialist machines are required, and therefore SMCs are appropriate.

Feedback Control Strategy On The Input Side Of Mc

Pulse Width Modulation

3.1 Pwm Techniques:

The inverter output voltage has been varied to the loading constraint. Whenever DC input voltage changes, the output voltage also changes. Hence these variations have to be accounted. In the case of motor drives the ratio of voltage to frequency (v/f) is maintained constant. The output voltage frequency of' the inverter are adjusted to remain v/f constant. Similarly, in UPS the output voltage of the inverter is to be regulated. These all the reasons indicate that the output voltage of the inverter has to be regulated.

The PWM techniques are primarily used for voltage control and able to control the switching devices of the drives.

- Single pulse width modulation techniques
- Multiple pulse width modulation techniques
- Sinusoidal pulse width modulation techniques
- Modified sinusoidal pulse width modulation techniques
- Phase displacement control techniques
- Space vector modulation techniques

From the above techniques, SPWM techniques and SVPWM are widely used. This thesis is proposed using SPWM and SVPWM techniques for USMC based WECS. The PWM techniques are used to control the output voltage of the inverter and the harmonics of the inverter.

3.1.1 SINGLE PULSE WIDTH MODULATION:

In single pulse width, modulation control technique consists single pulse for each half cycle. Figure 3.13 shows single pulse width modulation technique. The size of the single pulse has been adjusted to regulate the output voltage of the inverter. The rectangular reference signal of the amplitude (A_r) and a triangular carrier wave (A_c) are compared, and the gating signals are generated as shown in Figure 3.13. The output of the single phase full bridge inverter is regulated using the gating signal. The frequency of the reference signal has been used to determine the fundamental frequency of the output voltage.

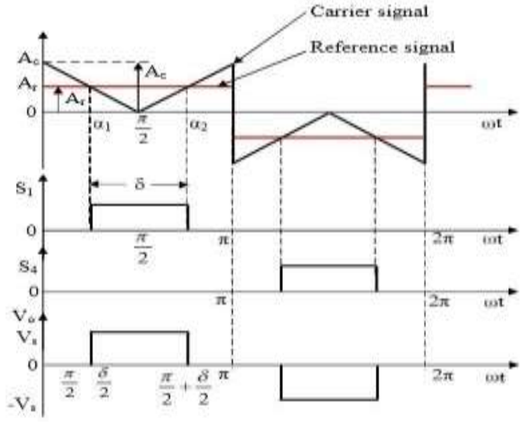

Fig 3.1 Generation of single pulse width modulation

Here as the instantaneous output voltage of the inverter is given by

$$Vo = V_s (S_1 - S_4)$$

This modulation provides quasi-square wave output. The signals have the single pulse during the output voltage of the each half cycle. The output voltage of the RMS value has been regulated using the varying pulse width

Multiple Pulse Width Modulation:

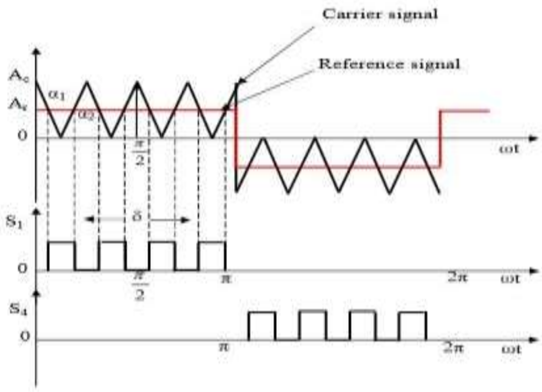

Fig 3.2 Generation of multiple pulse width modulation

The main problem of single PWM technique causes high harmonic content. Harmonic content is reduced by several pulses in each half cycle of the output voltage in the multiple PWM technique.

The production of gating signal is accomplished by comparing the reference signal of the amplitude (A_r) and the triangular carrier wave (A_c) as shown Figure 3.14. The frequency of the reference signal utilized for determining the output frequency. The modulation index used to control the output voltage of the inverter. Amount of pulses per half cycle is found by p

$$p = \frac{f_c}{2f_o}$$

$$= \frac{m_f}{2}$$

$$m_f = \frac{f_c}{f_o}$$

Where m_f is called as frequency modulation ratio

The instantaneous output voltage of the inverter is given by Vo $= V_s (S_1 - S_4)$

Conventional Control Method:

The indirect matrix converter (IMC), which is composed of a rectifier stage and an inverter stage, serves as the AC-AC power converter between power supply and load. IMC can also be replaced by direct matrix converter (DMC) since they have the same function [1] .

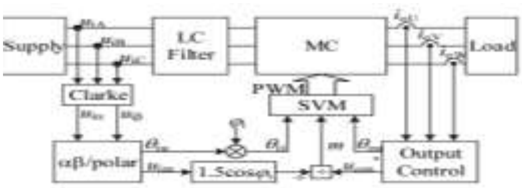

Fig 4.1 The conventional control method of feedforward compensation with fixed input power factor angle

The principle of the conventional control method presented in [10] is shown in Fig.4.1. The three-phase input voltages u_{iA}, u_{iB}, u_{iC} are sampled to calculate their αβ-axis components $u_{i\alpha}$ and $u_{i\beta}$ via Clarke transformation. Based on polar transformation, the instantaneous amplitude u_{im} and phase angle θ_{iu} of input voltage vector are got.

The input power factor angle φ_i which is usually fixed at 0 for unit power factor operation is added into θ_{iu}, and then the phase angle θ_{ii} of input current is obtained. U_{om} and θ_{ou} are the amplitude and phase angle of the expected output voltage vector separately, which are generated by open-loop or closed-loop output control. The modulation index u_{im} u_{om} *, and φ_i. After m, θ_{ii}, and θ_{ou} are obtained, the space vector modulation (SVM) algorithm can be implemented in digital controller [21].

4.2 Improved Control Method To Make Input Reference Currents Modifiable:

Fig. 4.1 shows that when the conventional control method generates the modulation signals m, θ_{ii}, and θ_{ou}, only the phase angle θ_{ii} of input current vector is directly controlled, but not the amplitude. This is the reason why MC doesn't allow for the feedback control of input currents [1, 6, 22]. Reference [20] presents an improved control method, of which the principle is illustrated in Fig. 3. In this method, the output control produces the expected value P_i* of active power and the dc bus current i_{dc} defined in [20]:

$$P_i^* = 1.5\left(u_{o\alpha}^* i_{o\alpha} + u_{o\beta}^* i_{o\beta}\right) \qquad (1)$$

$$i_{dc} = \frac{\sqrt{3}\left(u_{o\alpha}^* i_{o\alpha} + u_{o\beta}^* i_{o\beta}\right)}{2u_{om}^*} \qquad (2)$$

Where $u_{o\alpha}$* and $u_{o\beta}$* are the αβ-axis components of output reference voltages; $i_{o\alpha}$ and $i_{o\beta}$ are the αβ-axis components of output currents. P_i* and i_{dc} can also calculated in rotating frame. Based on instantaneous power theory [23], the input

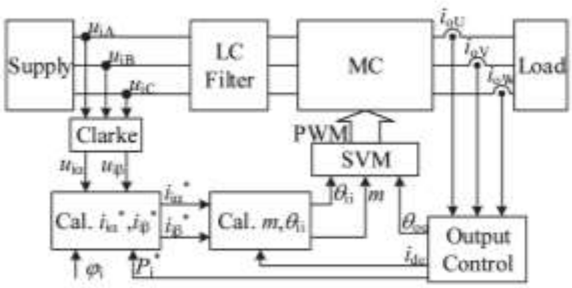

Fig 4.2 improved control method of MC

reference currents $i_{i\alpha}^*$ and $i_{i\beta}^*$btained from (1):

International Journal of Research
Available at https://journals.pen2print.org/index.php/ijr/
e-ISSN: 2348-6848
p-ISSN: 2348-795X
Volume 06 Issue 07
June 2019

$$\begin{cases} i_{i\alpha}^{*} = \dfrac{P_i^{*}\left(u_{i\alpha} - \tan\varphi_i u_{i\beta}\right)}{1.5\left(u_{i\alpha}^2 + u_{i\beta}^2\right)} \\ i_{i\beta}^{*} = \dfrac{P_i^{*}\left(u_{i\beta} + \tan\varphi_i u_{i\alpha}\right)}{1.5\left(u_{i\alpha}^2 + u_{i\beta}^2\right)} \end{cases} \quad (3)$$

After $i_{i\alpha}^*$ and $i_{i\beta}^*$ are got, the modulation index m and the input current vector angle θ_{ii} can be calculated [20]:

$$\begin{cases} m = \sqrt{\left(\dfrac{i_{i\alpha}^{*}}{i_{dc}}\right)^2 + \left(\dfrac{i_{i\beta}^{*}}{i_{dc}}\right)^2} \\ \theta_{ii} = \mathrm{atan2}\left(\dfrac{i_{i\beta}^{*}}{i_{dc}}, \dfrac{i_{i\alpha}^{*}}{i_{dc}}\right) \end{cases} \quad (4)$$

According to the analysis in [20], the improved control method shown in Fig.4.2 has exactly the same input-output transfer function with the conventional control method shown in Fig.4.1. However, the improved method could directly control the αβ-axis components (equivalently the amplitude and phase angle) of input currents. Therefore, it enables the realization of some input control strategies which require input currents to be directly controllable. For example, reference [20] modified the input reference currents with the derivations of actual values, realizing a novel active damping control strategy on the input side which has the same damping performance with passive damping control.

Block Diagram Of The Proposed Control Strategy:

Since the improved control method shown in Fig.4.2 completely controls the input currents, a feedback control strategy on the input side of MC is developed by this paper, which is shown in Fig.4.3. Fig.4.3(a) is the control block of the whole system while Fig. 4.3(b) illustrates the detailed structure of the input control strategy. As it can be seen from Fig.4.3, the input control includes closed-loop control of input active power and input currents. $G_P(s)$ and $G_I(s)$ are the controllers on the forward path respectively, while $F_P(s)$ and $F_I(s)$ are the controllers on the feedback path separately.

The closed-loop control of input active power produces the modified reference values P_i^{**}, which are used to replace P_i^* in (3) to calculate the input reference currents $i_{i\alpha}^*$ and $i_{i\beta}^*$. The closed-loop control of input currents produces the modified input reference currents $i_{i\alpha}^{**}$ and $i_{i\beta}^{**}$, which are used to replace $i_{i\alpha}^*$ and $i_{i\beta}^*$ in (4) to calculate the modulation signals m and θ_{ii}. In Fig. 4.3, the actual input active and reactive power are calculated based on instantaneous power theory [23];

$$P_i = 1.5\left(u_{i\alpha} i_{i\alpha} + u_{i\beta} i_{i\beta}\right)$$

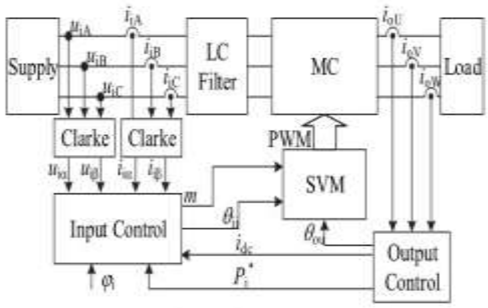

(a) System control block diagram

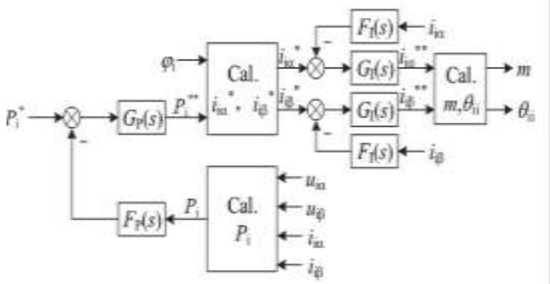

(b) Input control block diagram

Fig 4.3 feedback control strategeyon the input side of MC

It is noted that the control strategy is given in stationary frame, so as to maintain the consistence of this paper, but it is certainly applicable to the rotating frame.

Fig.4.3 shows that the feedback control on the input side is the inner-loop of the whole system control, while the output control is the outer-loop. Therefore, by designing appropriate controllers in the inner-loop, it is possible to achieve some control objects on the input side without affecting the output performance. In Fig. 4(b), the closed-loop control of input currents is similar to that in voltage source

e-ISSN: 2348-6848
p-ISSN: 2348-795X
Volume 06 Issue 07
June 2019

converters. However, the closed-loop control of input active power is specially designed for MC since its function is to maintain the active power constant as required by load, in case that the input current control influences the constant active power absorbed by load.

It should be stated here that the conventional control method shown in Fig.1.1 can achieve satisfactory input performance under ideal conditions, and thus it is unnecessary to adopt the input feedback control strategy shown in Fig.4. Nevertheless, in some cases, the input performance can be enhanced by the feedback control. For example, the feedback control strategy is applied to eliminate the input current harmonics under unbalanced input voltages, which will be introduced in chapter 5

Elimination Of Input Current Harmonics Under Unbalanced Input Voltages

In this section, the feedback control strategy shown in Fig. 4 is used to eliminate the input current harmonics caused by unbalanced input voltage. Part A introduces the harmonic distribution of input currents under unbalanced input voltages.

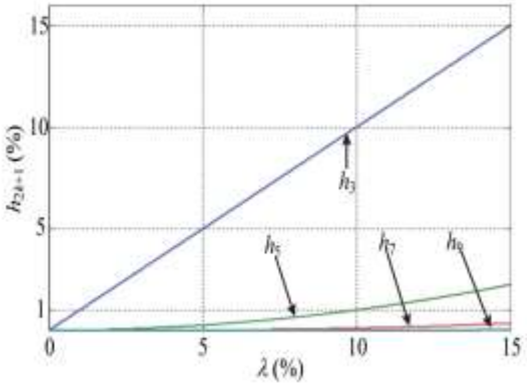

Fig 5.1 the harmonic contents h_{2k-1} in input currents with the conventional control method,when the unbalanced degree λ varies from 0-15%

Part B and Part C present the controller design for the closed-loop control of input currents and active power respectively. Part D proves that closed-loop control of input active power doesn't affect the performance of input current control. To simplify the control strategy, the input power factor angle φ_i is fixed at 0.

5.1 INPUT CURRENT HARMONICS WITH CONVENTIONAL CONTROL METHOD:

Supposing the input voltages are sinusoidal, the □□-axis components can be expressed as [15]

$$\begin{cases} u_{\alpha} = U_{ip}\cos(\omega_i t+\varphi_{iup})+U_{in}\cos(\omega_i t-\varphi_{iun}) \\ u_{\beta} = U_{ip}\sin(\omega_i t+\varphi_{iup})-U_{in}\sin(\omega_i t-\varphi_{iun}) \end{cases} \quad (6)$$

where U_{ip} and φ_{iup} are the amplitude and phase angle of positive sequence voltage, while U_{in} and φ_{iun} are the amplitude and phase angle of negative sequence voltage; ω_i is the input voltage frequency. U_{in} is 0 if input voltages are balanced and is nonzero otherwise. By substituting (6) into (3) and analyzing the spectrum, the input reference currents can be expressed in the form of Fourier series [11]:

$$\begin{cases} i_{i\alpha}^* = \dfrac{P_i^* \sum_{k=0}^{\infty}(-\lambda)^k \cos[(2k+1)\omega_i t+\varphi_{iuk}]}{1.5U_{ip}} \\ i_{i\beta}^* = \dfrac{P_i^* \sum_{k=0}^{\infty}(-\lambda)^k \sin[(2k+1)\omega_i t+\varphi_{iuk}]}{1.5U_{ip}} \end{cases} \quad (7)$$

where φ_{iuk} is phase angle of the $(2k+1)^{th}$ current harmonic; symbol λ is equal to U_{in} / U_{ip}, representing the unbalanced degree of input voltages.

According to Fig. 4.2, the conventional control method of feedforward compensation with fixed input power factor angle results in a lot of odd harmonics in the reference values of input currents, which are directly transferred into the actual values and thus lead to the degraded input power quality. In addition, as shown by (7), the ratio of the amplitude of $(2k+1)^{th}$ harmonic component to that of the fundamental component is denoted as h_{2k+1}:

$$h_{2k+1} = \lambda^k \quad (8)$$

Therefore, h_{2k+1} is a power function of the unbalanced degree . Besides, h_{2k+1} drops exponentially with the harmonic order,since is generally less than 1.

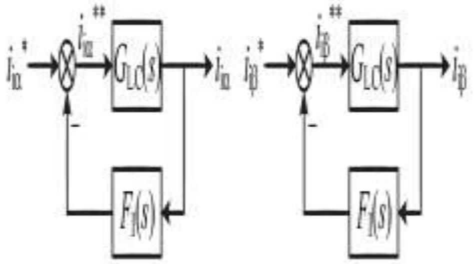

Fig 5.2 signal flow graph of closed loop control of αβ-axis input currents

In practice, the unbalanced degree λ of the grid voltages is usually less than 2% [24], but it could increase to more than 5% under abnormal condition. In this paper, the maximum of λ is supposed to be 15%, which could cover most practical cases. According to (8), when λ varies in the range of [0, 15%], the values of h_3, h_5, h_7, and h_9 which represent the contents of 3^{rd}, 5^{th}, 7^{th} and 9^{th} harmonics are shown in Fig.5.1. From Fig.5.1, it is clear that the 3^{rd} harmonic is primary in the whole range. When λ increases, h_5 goes up to 2.25% which is also noticeable. On the contrary, h_7 and h_9 are less than 0.5% which are ignorable in the whole range. To sum up, the conventional control method results in many 3^{rd} and 5^{th} input current harmonics which are necessary to be eliminated.

5.2 CONTROLLER DESIGN FOR THE INPUT CURRENT LOOP:

According to the discussion in part A, the input reference currents with conventional control method contain considerable 3rd and 5th harmonics, which will directly be transferred into the actual currents. To eliminate the current harmonics, resonant controllers are applied to the closed-loop control of input currents. The designed controllers $G_I(s)$ and $F_I(s)$ are

$$G_I(s)=1,\ F_I(s)=\frac{K_{RI3}s}{s^2+(3\omega_i)^2}+\frac{K_{RI5}s}{s^2+(5\omega_i)^2} \qquad (9)$$

Namely the forward path is directly feed through while the feedback controller $F_I(s)$ is composed of two resonant controllers in parallel, whose center frequencies are $3\omega_i$ and $5\omega_i$ respectively, and proportional coefficients are K_{RI3} and K_{RI5}. Certainly, if the contents of 7^{th} and 9^{th} harmonics are also significant, resonant controllers whose center frequencies are 7^{th} and 9^{th} can be incorporated into $F_I(s)$ to eliminate these harmonics. However, as it can be seen from (8) and Fig. 5.1, the harmonic contents of 7^{th} and above are less than 0.5% even when the unbalanced degree λ is up to 15%. Therefore, only the two controllers in (9) are adopted in this paper.

Ignoring the time-delay effect generated by PWM control of MC, the signal flow graphs of the closed-loop control of αβ-axis input currents are shown in Fig. 5.2. From Fig.5.2, the closed-loop transfer function of input currents is

$$H_I(s)=\frac{G_{LC}(s)}{1+F_I(s)G_{LC}(s)} \qquad (10)$$

where $G_{LC}(s)$ is the open-loop transfer function and is decided by the input LC-filter:

$$G_{LC}(s)=\frac{\frac{L_f}{R_d}s+1}{L_fC_fs^2+\frac{L_f}{R_d}s+1} \qquad (11)$$

According to (9) and (11), the gains of $F_I(s)$ at the frequency of $3\omega_i$ and $5\omega_i$ are infinite [25] while the gains of $G_{LC}(s)$ at these

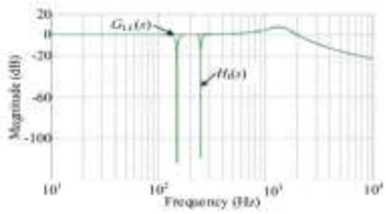

fig 5.3 frequency response of $G_{LC}(s)$ and $H_I(s)$

two frequencies are approximately unit. As a result, the gains of $H_I(s)$ at these two frequencies are zero, which can also be found from the frequency response of $H_I(s)$ shown in Fig.5.3. To highlight the control performance of $H_I(s)$, the frequency response of $G_{LC}(s)$ is also shown in Fig.5.3. It can be seen from Fig. 7 that compared with $G_{LC}(s)$, $H_I(s)$ reduces the gains at $3\omega_i$ and $5\omega_i$ to zero without changing the gains at

International Journal of Research
Available at https://journals.pen2print.org/index.php/ijr/
e-ISSN: 2348-6848
p-ISSN: 2348-795X
Volume 06 Issue 07
June 2019

the fundamental frequency and high frequencies.

Therefore, the closed-loop control of input currents only eliminates the 3rd and 5th harmonics, but doesn't affect the fundamental components and the filtering performance of the LC filter.

5.3 CONTROLLER DESIGN FOR THE INPUT ACTIVE POWER LOOP:

According to the frequency response of $H_I(s)$, the closed-loop control of input currents can completely remove the 3rd and 5thharmonics. Ignoring other minor harmonics, the actual input currents $i_{i\alpha}$ and $i_{i\beta}$ only contain fundamental components, which can be expressed as [11]

$$\begin{cases} i_{i\alpha} = \dfrac{P_i^* \cos\left(\omega_i t + \varphi_{iup}\right)}{1.5U_{ip}} \\ i_{i\beta} = \dfrac{P_i^* \sin\left(\omega_i t + \varphi_{iup}\right)}{1.5U_{ip}} \end{cases} \tag{12}$$

By substituting (6) and (12) into (5) and performing some basic trigonometric function operation, the actual input active power P_i is obtained:

$$P_i = P_i^* + \Delta P_i \tag{13}$$

Where ΔP_i is the power disturbance and is expressed as:

$$\Delta P_i = \lambda P_i^* \cos\left(2\omega_i t + \varphi_{iup} - \varphi_{iun}\right) \tag{14}$$

Therefore, the actual input active power P_i is not equal to its reference value P_i^* , but is equal to P_i^* added with an accomponent, whose frequency is $2\omega_i$ and amplitude is proportional to P_i^* and the unbalanced degree λ. (13) shows that although the input current feedback control can eliminate the 3rd and 5th current harmonics, it results in the harmonic of $2\omega_i$ in input active power.

Due to the absence of dc bus energy storage elements, this active power harmonic could directly be transferred to the output side, degrading the waveform quality of output currents.

To maintain the output performance, the resonant controller is further applied to the input active power feedback control. Similar to the input current feedback control, the resonant controller is also located in the feedback path, namely

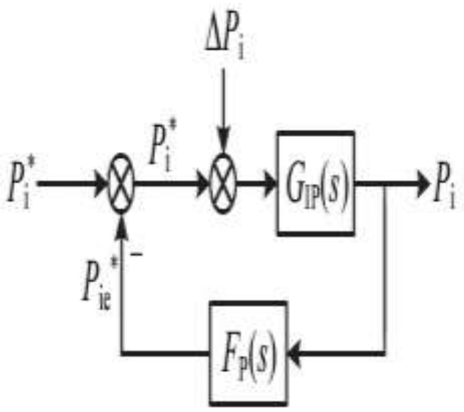

Fig 5.4 signal flow graph of closed loop control of input active power

$$G_P(s)=1,\ F_P(s)=\frac{K_{RP}s}{s^2+(2\omega_i)^2} \tag{15}$$

where K_{RP} is the proportional coefficient of $F_P(s)$. According to Fig.4.3(b) and (13), Fig.5.4 shows the signal flow graph of closed-loop control of input active power. In Fig.5.4, P_{ie}* is the additional control signal generated by the feedback controller $F_P(s)$. $G_{IP}(s)$ is the open-loop transfer function from P_i* and ΔP_i to the active power P_i, which is decided by the input current control. In (13), $G_{IP}(s)$ is ignored since only the steady-state value of active power is considered. However, in Fig. 8, $G_{IP}(s)$ is added into the signal flow graph so as to analyze the closed-loop transfer function $H_P(s)$ of active power. From Fig.5.4, the expression of $H_P(s)$ is

$$H_P(s)=\frac{G_P(s)}{1+F_P(s)G_P(s)} \tag{16}$$

It can be found from (15) and (16) that the gain of $H_P(s)$ at $2\omega_i$ is zero due to the infinite gain of $F_P(s)$ at $2\omega_i$, regardless of the gain of $G_{IP}(s)$ at $2\omega_i$. Therefore, the power disturbance ΔP_i of $2\omega_i$ cannot be transferred to the actual input active power. This means that the closed-

e-ISSN: 2348-6848
p-ISSN: 2348-795X
Volume 06 Issue 07
June 2019

loop control of input active power can eliminate the power harmonic caused by the closed-loop control of input currents and thus the waveform quality of output currents could be maintained.

Effect Of Active Power Control On The Input Current Control:

In the analysis of input current feedback control in part B, the effect of closed-loop control of input active power is not considered. Namely, the modified active power P_i^{**} generated by the active power control loop is assumed to be constant, just the same with the unmodified value P_i^*. This part proves thatthe assumption is reasonable. Since $F_P(s)$ has infinite gain at $2\omega_i$, the additional controlsignal P_{ie}^* output by it could completely compensate the powerdisturbance ΔP_i caused by the input current control.Consequently, P_{ie}^* is equal to ΔP_i at the steady state. According to Fig.5.4 and (14), the modified active power P_i^{**} at steady state can be written as

$$P_i^{**} = P_i^* - P_{ie}^* = P_i^* - \lambda P_i^* \cos\left(2\omega_i t + \varphi_{ium} - \varphi_{iim}\right) \quad (17)$$

Obviously, P_i^{**} contains an ac component whose frequency is$2\omega_i$. With P_i^* in (3) replaced by P_i^{**} and $\varphi_i=0$ substituted into(3), the input current reference values $i_{i\alpha}^*$ and $i_{i\beta}^*$

$$\begin{cases} i_{i\alpha}^* = \dfrac{P_i^* u_{i\alpha}}{1.5\left(u_{i\alpha}^2 + u_{i\beta}^2\right)} - \dfrac{P_{ie}^* u_{i\alpha}}{1.5\left(u_{i\alpha}^2 + u_{i\beta}^2\right)} \\ i_{i\beta}^* = \dfrac{P_i^* u_{i\beta}}{1.5\left(u_{i\alpha}^2 + u_{i\beta}^2\right)} - \dfrac{P_{ie}^* u_{i\beta}}{1.5\left(u_{i\alpha}^2 + u_{i\beta}^2\right)} \end{cases} \quad (18)$$

According to (3) and (7), the Fourier series of the first items on the right hand of the equations in (18) are composed of the 3rd, 5th, and other odd harmonics in addition to the fundamental components. Considering that the frequency of P_{ie}^* is $2\omega_i$, it iseasy to find that the second term on the right hand of equation (18) also contains 3rd, 5th, and other odd harmonics. Therefore, the input active power feedback control changes the contents of the odd harmonics in the input reference currents $i_{i\alpha}^*$ and $i_{i\beta}^*$, but does not generate harmonics of new orders. From the view point of input current feedback control, the modified active power reference P_i^{**} with ac component whose frequency is $2\omega_i$ has no difference with the unmodified constant value P_i^*, since the closed-loop control of input currents can remove the odd harmonics completely.

Simulation And Experimental Verification

Simulation And Experimental Results

In order to verify the effectiveness of the proposed control strategy, an IMC prototype is built by this paper and a corresponding simulation model is constructed in the MATLAB/Simulink software.

λ(%)	U_{iA}(V)	U_{iB}(V)	U_{iC}(V)	U_p(V)	U_n(V)
0	169.7	169.7	169.7	169.7	0.0
5	155.0		184.4		8.5
10	140.3		199.1		17.0
15	125.4		214.0		25.5

Table 1 amplitudes of the three phase voltages and the positive and negative sequence voltages under different unbalanced degrees

To produce the unbalanced input voltages, a programmable AC power source is selected as the power supply of IMC. In simulation and experiments, the input frequency is 50Hz, and the phase difference between each two phases is 120°. The amplitude of phase-B input voltage is fixed at 169.7V (corresponding to RMS 120V). Different unbalanced degrees are achieved by changing the amplitudes of the other two phases. The amplitudes of three phases input voltages, the positive sequence voltages, and the negative sequence voltages under different unbalanced degrees are shown in Table I.

The parameters of the experimental prototype are shown in Table 2. In experiments, the commonly used current feedback control in rotating frame is applied to the output side.

e-ISSN: 2348-6848
p-ISSN: 2348-795X
Volume 06 Issue 07
June 2019

The output frequency is 80Hz and the reference amplitude of the output currents is fixed at 10A. The SVM of symmetrical switching pattern is applied to IMC, resulting in different switching frequencies of the rectifier stage and inverter stage, which are 10 kHz and 20 kHz separately.

In simulation model, the power switches of IMC are ideal, the control method is realized by Simulink modules, and the rest parameters are the same with those shown in Table II.

Variables	Description	Values
Input LC Filter		
L_f	Filter Inductor	1mH
C_f	Filter Capacitor	12.6μF
R_d	Damping Resistor	19Ω
IMC Power Setup		
IGBT	Power Module of Rectifier Stage	APTGT50TDU60PG
Module	Power Module of Inverter Stage	PM75RLA060
Load		
L_L	Load Inductor	2mH
R_L	Load Resistor	7Ω
F_o	Output Frequency	80Hz
Controller		
DSP	Digital Signal Processor	TMS320F28335
CPLD	Complex Programmable Logic Device	EPM1270T144C8N
ADC	Analog-to-Digital Converter	ADS8568
DAC	Digital-to-Analog Converter	AD5438
$f_{sampling}$	Sampling Frequency	20 kHz
$f_{switching}$	Switching Frequency of Rectifier Stage	10 kHz
	Switching Frequency of Inverter Stage	20 kHz

Table 2 parameters of the experimental prototype

SIMULATION RESULTS:

Fig 6.1shows the simulation results. Three-phase input voltages are illustrated in Fig. 6.1 (a). The total simulation time is 0.2s. The input voltages are balanced in the first 0.1s while are unbalanced in the last 0.1s with an unbalanced degree of 15%. Fig. 6.1(b) and Fig. 6.1(c) show the output currents with conventional control method and the proposed strategy respectively. From these two sub-figures, it is found that the output currents with the two methods are all sinusoidal no matter whether the input voltages are balanced or not. Fig. 6.1 (d) and Fig. 6.1(e) show the input currents. When input voltages are balanced, the input currents are sinusoidal with both methods. However, in the unbalanced case, the input currents are severely distorted with the conventional control method, but are sinusoidal with the proposed strategy. In summary, the simulation results prove that compared with the conventional control method, the proposed strategy can improve the input currents dramatically while maintain the waveform quality of output currents.

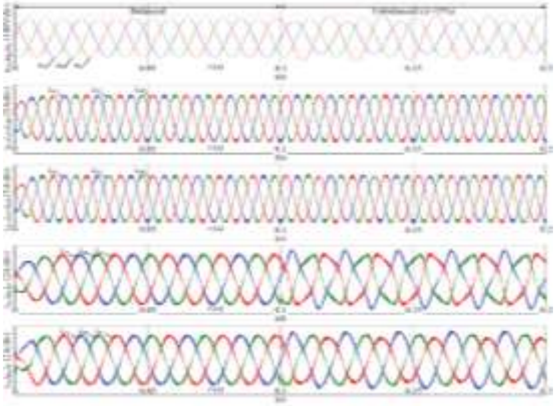

Fig 6.1 simulation results (a) input voltages;(b) Output currentsvwith conventional control method ;(c) Output currents with the proposed control strategy;(d) input currents with conventional control method;(e) input currents with the proposed control strategy

EXPERIMENTAL RESULTS:

In experiments, the dc bus voltage, input and output currents are measured with voltage probes and current probes separately whose bandwidths are 30MHz. The measured data are also used for harmonic analysis in the MATLAB software.

Fig. 6.2 shows the three-phase output currents and the harmonic distributions of phase-U output current with the conventional control method and the proposed strategy, when the unbalanced degree of input voltages is 15%. In addition, the waveform of the dc-bus voltage udc is also given in Fig. 6.2, so as to indicate that the input voltages are unbalanced. As can be seen from Fig. 6.2, the contents of low order harmonics in output currents with the two control methods are less than 0.5%, even if the unbalanced degree of input voltages is up to 15%, showing satisfactory waveform quality.

The total harmonic distortion (THD) of output currents is larger than 3.0% due to the high order harmonics around the switching frequency, which can be reduced by increasing the value of load inductor or switching frequency.

Fig. 6.3 shows the input currents and the harmonic distribution of phase-A input current with the two control methods. With the conventional control method, the THD of input current is up to 15.02%, the content of 3rd harmonic is about 15%, and the content of 5th harmonic is about 2%, which is corresponding to the theoretical analysis in Section III Part A. On the contrary, the THD of input current drops to 3.40% by adopting the proposed control strategy. In particular, the contents of the major low-order harmonics are less than 1%, indicating that sinusoidal input currents are obtained. The high order harmonics contribute to the THD of input currents, which can be reduced by increasing the damping resistor Rd [26] or by applying active damping control strategy [20], [22], [27].

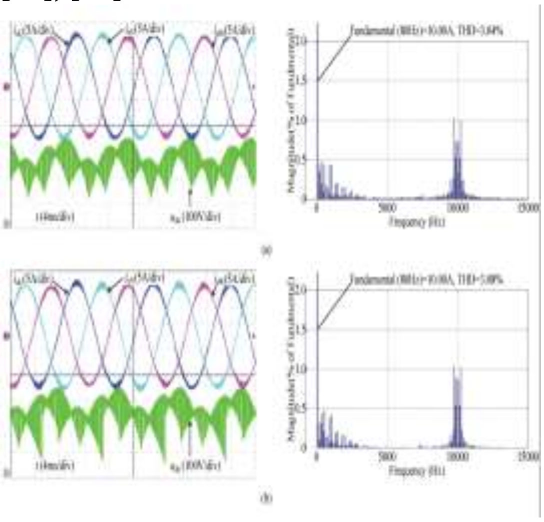

Fig 6.2 when the unbalanced degree of input voltages is 15%,waveforms of output currents ($i_{\alpha U}$ $i_{\alpha V}$ $i_{\alpha W}$)dc bus voltage(u_{dc})and the harmonic distribution of phase U output current (a) with conventional control method(b)with the proposed strategy

The conventional control method and the proposed strategy are further comparatively evaluated under different unbalanced degree of input voltages. The waveforms of output currents with both methods are almost the same with those shown in Fig. 6.3,

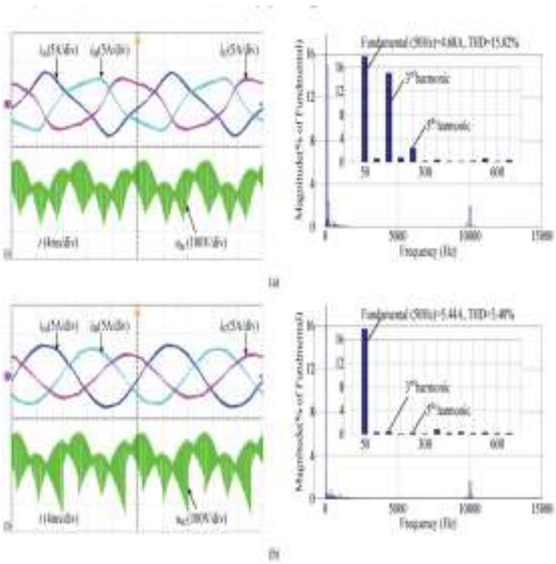

Fig 6.3 when the unbalanced degree of input voltages is 15%,waveforms of input currents ($i_{\alpha A}$ $i_{\alpha B}$ $i_{\alpha C}$)dc bus voltage(u_{dc}) and the harmonic distribution of phase U output current (a) with conventional control method (b)with the proposed strategy

but the waveforms of input currents are different which are presented in Fig. 6.4 and Fig. 6.5. By comparing Fig. 6.4 and Fig. 6.5, it can be found that the input currents with conventional control method become more and more distorted with the increase of unbalanced degree λ. On the contrary, the input currents with the proposed method maintain sinusoidal when λ varies

The harmonic analysis results of output currents and input currents are shown in Fig. 6.6. It is found from Fig. 6.6(a) that both the two methods can achieve satisfactory waveform quality of output currents when the unbalanced degree varies from 0% to 15%, since the THDs are all around 3.0%. Fig. 6.6(b) shows the THDs of input currents with the two control methods

International Journal of Research
Available at https://journals.pen2print.org/index.php/ijr/

e-ISSN: 2348-6848
p-ISSN: 2348-795X
Volume 06 Issue 07
June 2019

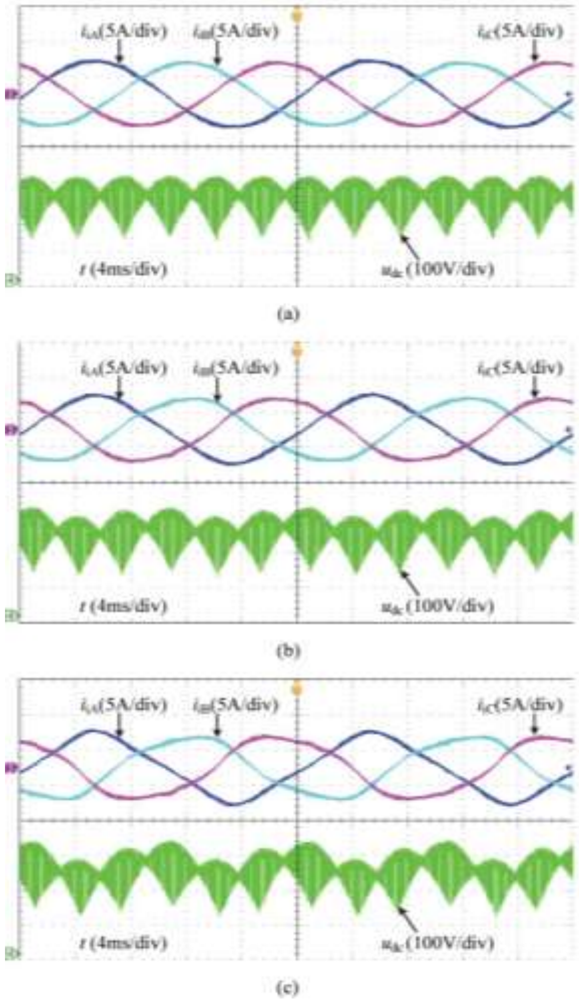

Fig 6.4 waveforms of the input currents(i_{iA} i_{iB} i_{iC}) and dc bus voltge u_{dc} with the conventional control method under different unbalanced degree λ:(a) λ=0(input voltages are balanced) (b)λ=5% (c)λ=10%

It is clear that the THD of input current with the conventional control method increases rapidly to 15%, but keeps below 4% with the proposed control strategy. According to the analysis in Section III, the 3rd and 5th harmonics are the primary harmonics, and thus they are illustrated in Fig. 6.8(c) and (d).

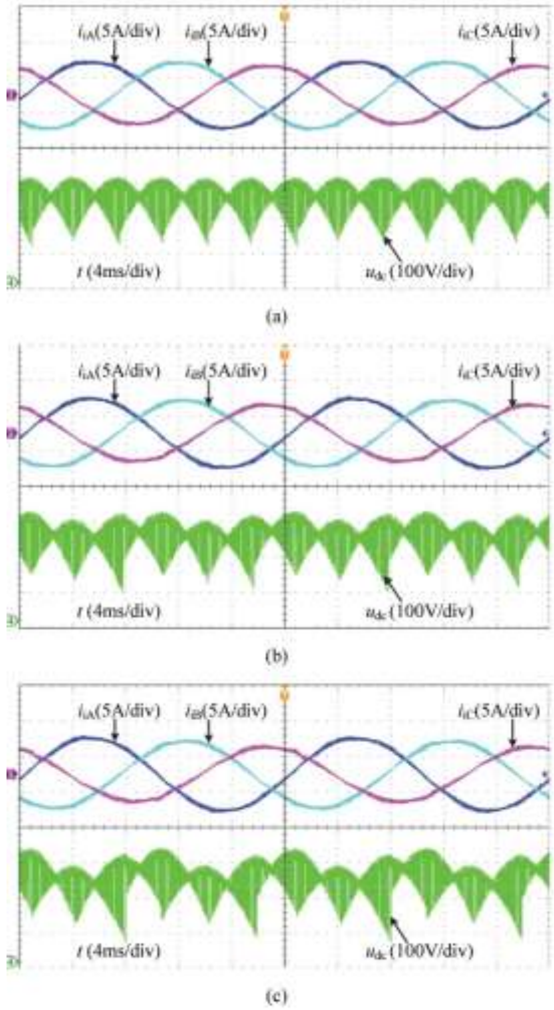

Fig 6.5 waveforms of the input currents(i_{iA} i_{iB} i_{iC}) and dc bus voltge u_{dc} with the praposed control method under different unbalanced degree λ:(a) λ=0(input voltages are balanced) (b)λ=5% (c)λ=10%

With the increasing unbalanced degree λ, the contents of the 3rd and 5th harmonics with conventional control method both go up at the rate similar with that shown in Fig.6.6, but are suppressed to 1% and lower with the proposed control strategy

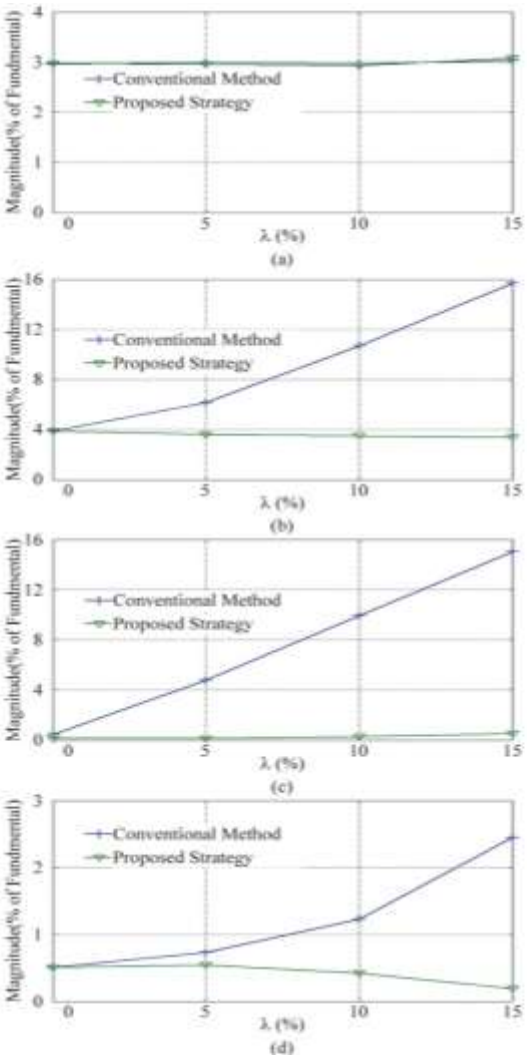

Fig 6.6 when the unbalanced degree of input voltages varies in the range 0-15%, the harmonic contents of phase U output current and phase A input current with the conventional control method and the proposed strategy;(a)THD of output current (b)THD of input current (c)content of 3rd harmonic to input current (d) content of 5th harmonic to input current

CONCLUSION

The feedback control strategy on the input side of MC is proposed by this paper based on a control method which enables input reference currents to be modifiable. This control strategy includes closed-loop control of input currents and input active power. By designing appropriate controllers, the input control object can be achieved without degrading the output performance. The proposed control strategy not only addresses the issue that closed-loop control of input currents is difficult to realize, but also helps to increase the degree of freedom and robustness of MC.

This project then adopts the proposed control strategy to eliminate the input current harmonics under unbalanced input voltages, with resonant controllers designed in the active power loop and input current loop. By applying the proposed control strategy, sinusoidal input currents are obtained, while waveform quality of output currents is maintained. The simulation and experimental results demonstrate that the proposed strategy obtains sinusoidal input currents while maintains good waveform quality of output currents, when the unbalanced degree of input voltages is up to 15%.

REFERENCE

[1] T. Friedli, J. W. Kolar, J. Rodriguez, and P. W. Wheeler, "Comparative evaluation of three-phase ac-ac matrix converter and voltage dc-link back-to-back converter systems," IEEE Trans. Ind. Electron., vol. 59, no. 12, pp. 4487–4510, Dec. 2012.

[2] L. Empringham, J. Kolar, J. Rodriguez, P. W. Wheeler, and J. C. Clare, "Technological issues and industrial application of matrix converters: A review," IEEE Trans. Ind. Electron., vol. 60, no. 10, pp. 4260–4271, Oct. 2013.

[3] S.S. Sebtahmadi, H. Pirasteh, S.H.A. Kaboli, A. Radan, and S. Mekhilef, "A 12-Sector Space Vector Switching Scheme for Performance Improvement of Matrix-Converter-Based DTC of IM Drive," IEEE Trans. Power. Electron., vol. 30, no. 7, pp. 3804-3817, July. 2015.

[4] J. Monteiro, J.F. Silva, S.F. Pinto, and J. Palma. "Linear and Sliding-Mode Control Design for Matrix Converter-Based Unified Power Flow Controllers," IEEE Trans. Power Electron. vol. 29, no. 7, pp. 3357-3367, Jul. 2014.

[5] X. Liu, P. C. Loh, P. Wang, F. Blaabjerg, Y. Tang, and E. A. Al-Ammar, "Distributed Generation Using Indirect Matrix Converter

in Reverse Power Mode," IEEE Trans. Power Electron., vol.28, no.3, pp.1072-1082, March 2013.

[6] J. Kolar, T. Friedli, J. Rodriguez, and P. W. Wheeler, "Review of three phase PWM ac-ac converter topologies," IEEE Trans. Ind. Electron., vol. 58, no.

[7] J. Haruna and J. Itoh, "Behavior of a Matrix Converter with a Feed Back Control in an Input Side," in Proc. IPEC., 2010, pp. 1202–1207.

[8] J. Haruna, J. Itoh: "Control Strategy for a Matrix Converter with a Generator and a Motor", in Proc. 26th IEEE APEC, 2011, pp. 1782-1789.

[9] V. Kumar and R. R. Joshi, "DSP-based matrix converter operation under various abnormal conditions with practicality," in Proc. IEEE PEDES Conf., vol. 2, pp. 1–4, Jan. 8–11, 1996.

[10] P. Nielsen, F. Blaabjerg, and J. K. Pedersen, "Space vector modulated matrix converter with minimized number of switchings and a feedforward compensation of input voltage unbalance," in Proc. PEDES'96, vol. 2, pp. 833–839, Jan. 8-11, 1996.

[11] D. Casadei, G. Serra, and A. Tani, "Reduction of the input current harmonic content in matrix converters under input/output unbalance," IEEE Trans. Ind. Electron., vol. 45, no. 3, pp. 401–411, Jun. 1998.

[12] X. Wang, H. Lin, H. She, and B. Feng, "A research on space vector modulation strategy for matrix converter under abnormal input-voltage conditions," IEEE Trans. Ind. Electron., vol. 59, no. 1, pp. 93–104, Jan. 2012.

[13] F. Blaabjerg, D. Casadei, C. Klumpner, and M. Matteini, "Comparison of two current modulation strategies for matrix converters under unbalanced input voltage conditions," IEEE Trans. Ind. Electron., vol. 49, no. 2, pp. 289–296, Apr. 2002.

[14] J. K. Kang, H. Hara, A. M. Hava, E. Yamamoto, E. Watanabe, and T. J. Kume, "The matrix converter drive performance under abnormal input voltage conditions," IEEE Trans. Power Electron., vol. 17, no. 5, pp. 721–730, Sep. 2002.

[15] Y. Yan, H. An, T. Shi, and C. Xia. "Improved double line voltage synthesis of matrix converter for input current enhancement under unbalanced power supply," IET Power Electron., vol. 6, no. 4, pp. 798-808, Apr. 2013.

[16] J.D. Dasika, and M. Saeedifard. "An Online Modulation Strategy to Control the Matrix Converter Under Unbalanced Input Conditions," IEEE Trans. Power Electron., vol. 30, no. 8, pp. 4423-4436, Aug. 2015.

[17] X. Li, M. Su, Y. Sun, H. Dan, and W.Xiong. "Modulation strategies based on mathematical construction method for matrix converter under unbalanced input voltages," IET Power Electron., vol. 6, no. 3, pp. 434-445, Mar. 2013.

[18] J. Lei, B. Zhou, J. Bian, X. Qin, and J. Wei, "A Simple Method for Sinusoidal Input Currents of Matrix Converter Under Unbalanced Input Voltages," IEEE Trans. Power Electron., vol. 31, no. 1, pp. 21–25, Jan. 2016.

[19] S. Li, X. Wang, Z. Yao, T. Li, and Z. Peng. "Circulating Current Suppressing Strategy for MMC-HVDC Based on Nonideal Proportional Resonant Controllers Under Unbalanced Grid Conditions," IEEE Trans. Power Electron., vol. 30, no. 1, pp. 387-397, Jan. 2015.

[20] J. Lei, B. Zhou, X. Qin, J. Wei, and J. Bian. "Active Damping Control Strategy of Matrix Converter via Modifying Input Reference Currents," IEEE Trans. Power Electron., vol. 30, no. 9, pp. 5260-5271, Sept. 2015.

[21] J. Rodriguez, M. Rivera, J. W. Kolar, and P. W. Wheeler, "A review of control and modulation methods for matrix converters," IEEE Trans. Ind. Electron., vol. 59, no. 1, pp. 58–70, Jan. 2012.

[22] Y. Sun, M. Su, X. Li, H. Wang, and W. Gui, "A general constructive approach to matrix converter stabilization," IEEE Trans.

Power. Electron., vol. 28, no. 1, pp. 418–431, Jan. 2013.

[23] H. Akagi, Y. Kanazawa, and A. Nabae, “Generalized theory of the instantaneous reactive power in three-phase circuits,” in Proc. IPEC, 1983, pp. 1375–1386.

[24] IEEE, “IEEE recommended practice for monitoring electric power quality,” IEEE Std 1159-2009 (Revision of IEEE Std 1159-1995), pp. c1–81, June 2009.

[25] D. N. Zmood and D. G. Holmes, “Stationary frame current regulation of PWM inverters with zero steady-state error,” IEEE Trans. Power Electron., vol. 18, no. 3, pp. 814–822, May 2003.

[26] J. Andreu, I. Kortabarria, E. Ormaetxea, E. Ibarra, J. L. Martin, and S. Apinaniz, “A step forward towards the development of reliable matrix converters,” IEEE Trans. Ind. Electron., vol. 59, no. 1, pp. 167–183, Jan. 2012.

[27] J. Lei, B. Zhou, X. Qin, J. Bian, and J. Wei, “Stability improvement of matrix converter by digitally filtering the input voltages in stationary frame,” IET Power Electron., E-First, Nov. 2015.